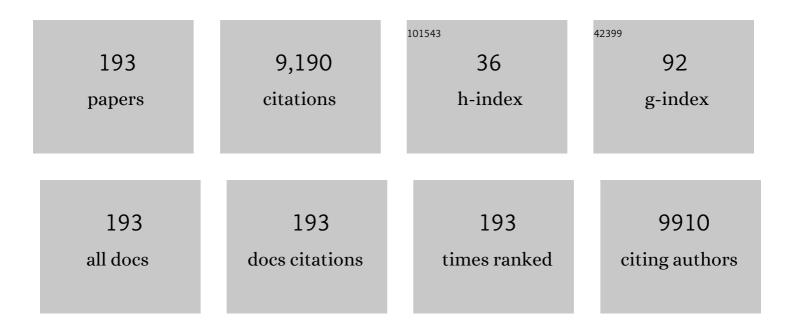
Sung Heum Park

List of Publications by Year in descending order

Source: https://exaly.com/author-pdf/335716/publications.pdf Version: 2024-02-01



#	Article	IF	CITATIONS
1	The biopolymer-assisted synthesis of assembled g-C ₃ N ₄ open frameworks with electron delocalization channels for prompt H ₂ production. Catalysis Science and Technology, 2022, 12, 1368-1377.	4.1	13
2	Enhanced phase separation in PEDOT:PSS hole transport layer by introducing phenylethylammonium iodide for efficient perovskite solar cells. Journal of Renewable and Sustainable Energy, 2022, 14, 013502.	2.0	3
3	Design and photovoltaic properties of conjugated polymers based on quinoxaline and diketopyrrolopyrrole for OSCs. Synthetic Metals, 2022, 285, 117016.	3.9	1
4	Up-conversion luminescence performance of Tm3+/Yb3+ co-doped strontium cerate phosphors. Optik, 2022, 262, 169264.	2.9	3
5	A polymer/small-molecule binary-blend hole transport layer for enhancing charge balance in blue perovskite light emitting diodes. Journal of Materials Chemistry A, 2022, 10, 13928-13935.	10.3	15
6	Photovoltaic Performances of Dye-Sensitized Solar Cells Based on Modified Polybutadiene Matrix Electrolytes by Sol-Gel Process. Polymers, 2022, 14, 2347.	4.5	2
7	Highly efficient and freely soluble titanium sub-oxide powder as interfacial functional material for versatile photovoltaic cells. Chemical Engineering Journal, 2022, 450, 138017.	12.7	0
8	Curvature effects of electron-donating polymers on the device performance of non-fullerene organic solar cells. Journal of Power Sources, 2021, 482, 229045.	7.8	12
9	Boosting the efficiency of quasi-2D perovskites light-emitting diodes by using encapsulation growth method. Nano Energy, 2021, 80, 105511.	16.0	54
10	Carrier losses in non-geminate charge-transferred states of nonfullerene acceptor-based organic solar cells. Spectrochimica Acta - Part A: Molecular and Biomolecular Spectroscopy, 2021, 250, 119227.	3.9	6
11	Improved exciton dissociation efficiency by a carbon-quantum-dot doped workfunction modifying layer in polymer solar cells. Current Applied Physics, 2021, 21, 140-146.	2.4	7
12	Ce 3+ /Tb 3+ â€coactived NaMgBO 3 phosphors toward versatile applications in white LED, FED, and optical antiâ€counterfeiting. Journal of the American Ceramic Society, 2021, 104, 5086-5098.	3.8	11
13	Ligand-engineered bandgap stability in mixed-halide perovskite LEDs. Nature, 2021, 591, 72-77.	27.8	471
14	Design and theoretical study of superlative quantum efficiency and thermal stability phosphor: The system of Sr9Eu(PO4)7. Journal of Alloys and Compounds, 2021, 862, 158285.	5.5	2
15	Self-reduction process of Eu3+ to Eu2+ in Eu-doped SrLaMgTaO6 double perovskite thin films and its photoluminescence properties. Optical Materials, 2021, 116, 111092.	3.6	8
16	In-situ intramolecular synthesis of tubular carbon nitride S-scheme homojunctions with exceptional in-plane exciton splitting and mechanism insight. Chemical Engineering Journal, 2021, 414, 128802.	12.7	48
17	Water-Repellent Perovskites Induced by a Blend of Organic Halide Salts for Efficient and Stable Solar Cells. ACS Applied Materials & Interfaces, 2021, 13, 33172-33181.	8.0	7
18	Enhanced Charge Separation in Ternary Bulk-Heterojunction Organic Solar Cells by Fullerenes. Journal of Physical Chemistry Letters, 2021, 12, 6418-6424.	4.6	10

#	Article	IF	CITATIONS
19	Influence of thiophene and furan π–bridge on the properties of poly(benzodithiophene-alt-bis(π–bridge)pyrrolopyrrole-1,3-dione) for organic solar cell applications. Polymer, 2021, 229, 123991.	3.8	9
20	Enhancement in charge extraction and moisture stability of perovskite solar cell via infiltration of charge transport material in grain boundaries. Journal of Power Sources, 2021, 506, 230212.	7.8	6
21	Small molecules based difluoroquinoxaline for organic solar cells. Molecular Crystals and Liquid Crystals, 2021, 728, 45-51.	0.9	0
22	Versatile control of concentration gradients in non-fullerene acceptor-based bulk heterojunction films using solvent rinse treatments. Green Energy and Environment, 2021, , .	8.7	2
23	<i>In situ</i> cadmium surface passivation of perovskite nanocrystals for blue LEDs. Journal of Materials Chemistry A, 2021, 9, 26750-26757.	10.3	18
24	Dual-functional of non-contact thermometry and field emission displays via efficient Bi3+ → Eu3+ energy transfer in emitting-color tunable GdNbO4 phosphors. Chemical Engineering Journal, 2020, 382, 122861.	12.7	173
25	Controllable Eu valence based on linear structural evolution in single-phased Sr3-La1+(PO4)3-(SiO4) phosphors to realize tunable/white light emissions. Journal of Alloys and Compounds, 2020, 817, 152743.	5.5	4
26	NUV light induced visible emission in Er ³⁺ â€activated NaSrLa(MoO ₄)O ₃ phosphors for green LEDs and thermometer. Journal of the American Ceramic Society, 2020, 103, 1174-1186.	3.8	17
27	Near-ultraviolet light induced red emission in Sm3+-activated NaSrLa(MoO4)O3 phosphors for solid-state illumination. Journal of Alloys and Compounds, 2020, 817, 152705.	5.5	61
28	Molecular aggregation method for perovskite–fullerene bulk heterostructure solar cells. Journal of Materials Chemistry A, 2020, 8, 1326-1334.	10.3	15
29	Water-stable polymer hole transport layer in organic and perovskite light-emitting diodes. Journal of Power Sources, 2020, 478, 228810.	7.8	6
30	Rational design of efficient near-infrared photon conversion channel via dual-upconversion process for superior photocatalyst. Carbon, 2020, 169, 111-117.	10.3	8
31	Design and synthesis of small molecules with difluoroquinoxaline units for OSCs. Molecular Crystals and Liquid Crystals, 2020, 705, 79-86.	0.9	0
32	Synthesis and photovoltaic properties of organic molecules based on difluoroquinoxaline derivatives for OPVs. Molecular Crystals and Liquid Crystals, 2020, 705, 57-64.	0.9	1
33	Bilateral Interface Engineering for Efficient and Stable Perovskite Solar Cells Using Phenylethylammonium Iodide. ACS Applied Materials & Interfaces, 2020, 12, 24827-24836.	8.0	27
34	Luminescence properties and energy transfer of Mn4+-doped double perovskite La2ZnTiO6 phosphor. Optical Materials, 2020, 106, 109980.	3.6	16
35	Achieving non-contact optical thermometer via inherently Eu2+/Eu3+-activated SrAl2Si2O8 phosphors prepared in air. Journal of Alloys and Compounds, 2020, 843, 155858.	5.5	45
36	Enhanced performance of ternary polymer solar cells via property modulation of co-absorbing wide band-gap polymers. Journal of Power Sources, 2020, 471, 228457.	7.8	6

#	Article	IF	CITATIONS
37	Eu3+-activated Ca3Mo0.2W0.8O6 red-emitting phosphors: A near-ultraviolet and blue light excitable platform for solid-state lighting and thermometer. Journal of Luminescence, 2020, 223, 117212.	3.1	23
38	2D Perovskite Seeding Layer for Efficient Airâ€Processable and Stable Planar Perovskite Solar Cells. Advanced Functional Materials, 2020, 30, 2003081.	14.9	48
39	Solution processable small molecules as efficient electron transport layers in organic optoelectronic devices. Journal of Materials Chemistry A, 2020, 8, 13501-13508.	10.3	19
40	Solution-processable ambipolar organic field-effect transistors with bilayer transport channels. Polymer Journal, 2020, 52, 581-588.	2.7	10
41	Lead Acetate Assisted Interface Engineering for Highly Efficient and Stable Perovskite Solar Cells. ACS Applied Materials & Interfaces, 2020, 12, 7186-7197.	8.0	20
42	Enhanced photovoltaic performance of benzodithiophene-alt-bis(thiophen-2-yl)quinoxaline polymers via π–bridge engineering for non-fullerene organic solar cells. Polymer, 2020, 194, 122408.	3.8	6
43	Theoretical design and characterization of high efficient Sr9Ln(PO4)7: Eu2+ phosphors. Materials Research Bulletin, 2020, 127, 110856.	5.2	8
44	Full-color tuning in europium doped phosphosilicate phosphors via adjusting crystal field modulation or excitation wavelength. Journal of Alloys and Compounds, 2019, 770, 411-418.	5.5	11
45	Full-color tuning by controlling the substitution of cations in europium doped Sr8-xLa2+x(PO4)6-x(SiO4) xO2 phosphors. Dyes and Pigments, 2019, 160, 145-150.	3.7	10
46	Cation substitution induced excellent quantum efficiency and thermal stability in (Ca1â^'xSrx)9La(PO4)7:Eu2+ phosphors. New Journal of Chemistry, 2019, 43, 12325-12330.	2.8	6
47	Oneâ€Pot Exfoliation of Graphitic C ₃ N ₄ Quantum Dots for Blue QLEDs by Methylamine Intercalation. Small, 2019, 15, e1902735.	10.0	26
48	Wide band-gap organic molecules containing benzodithiophene and difluoroquinoxaline derivatives for solar cell applications. Molecular Crystals and Liquid Crystals, 2019, 685, 29-39.	0.9	2
49	Controlled crystal facet of MAPbI ₃ perovskite for highly efficient and stable solar cell <i>via</i> nucleation modulation. Nanoscale, 2019, 11, 170-177.	5.6	42
50	Eu3+ doped (Li, Na, K) LaMgWO6 red emission phosphors: An example to rational design with theoretical and experimental investigation. Journal of Alloys and Compounds, 2019, 785, 651-659.	5.5	36
51	Study on Na3Lu1-xEux(PO4)2 phosphor: High efficient Na3Eu(PO4)2 red emitting phosphor with excellent thermal stability. Journal of Alloys and Compounds, 2019, 805, 346-354.	5.5	19
52	Infrared excited Er ³⁺ /Yb ³⁺ codoped NaLaMgWO ₆ phosphors with intense green up-conversion luminescence and excellent temperature sensing performance. Dalton Transactions, 2019, 48, 11382-11390.	3.3	34
53	Efficient Polymeric Donor for Both Visible and Near-Infrared-Absorbing Organic Solar Cells. ACS Applied Energy Materials, 2019, 2, 4284-4291.	5.1	6
54	Visible to Nearâ€Infraredâ€Absorbing Polymers Containing Bithiazole and 2,3â€Didodecylâ€6,7â€Difluoroquinoxaline Derivatives for Polymer Solar Cells. Bulletin of the Korean Chemical Society, 2019, 40, 686-690.	1.9	2

#	Article	IF	CITATIONS
55	Dual-functional light-emitting perovskite solar cells enabled by soft-covered annealing process. Nano Energy, 2019, 61, 251-258.	16.0	14
56	Application of thermally coupled energy levels in Er3+ doped CdMoO4 phosphors: Enhanced solid-state lighting and non-contact thermometry. Materials Research Bulletin, 2019, 117, 63-71.	5.2	28
57	Efficiency enhancements in non-fullerene acceptor-based organic solar cells by post-additive soaking. Journal of Materials Chemistry A, 2019, 7, 8805-8810.	10.3	19
58	Improved Adhesion of Metal Electrode Layer on Si ₃ N ₄ Substrate through an All-Wet Process. ECS Journal of Solid State Science and Technology, 2019, 8, P159-P164.	1.8	2
59	Simultaneous bifunctional application of solid-state lighting and ratiometric optical thermometer based on double perovskite LiLaMgWO ₆ :Er ³⁺ thermochromic phosphors. RSC Advances, 2019, 9, 7189-7195.	3.6	25
60	Enhanced Magnetic Properties of FeCo Alloys by Two-Step Electroless Plating. Journal of the Electrochemical Society, 2019, 166, D131-D136.	2.9	8
61	Open Atmosphere-Processed Stable Perovskite Solar Cells Using Molecular Engineered, Dopant-Free, Highly Hydrophobic Polymeric Hole-Transporting Materials: Influence of Thiophene and Alkyl Chain on Power Conversion Efficiency. Journal of Physical Chemistry C, 2019, 123, 8560-8568.	3.1	18
62	Syntheses and Properties of Random Copolymers Using Thienyl-Thieno-Indole and Bithiophene-Dicarboximide with Different Ratios. Macromolecular Research, 2019, 27, 470-475.	2.4	3
63	Hierarchical multi-level block copolymer patterns by multiple self-assembly. Nanoscale, 2019, 11, 8433-8441.	5.6	22
64	Side-chain influences on the properties of benzodithiophene-alt-di(thiophen-2-yl)quinoxaline polymers for fullerene-free organic solar cells. Polymer, 2019, 172, 305-311.	3.8	13
65	Er ³⁺ -Activated NaLaMgWO ₆ double perovskite phosphors and their bifunctional application in solid-state lighting and non-contact optical thermometry. Dalton Transactions, 2019, 48, 4405-4412.	3.3	74
66	Fluorescence spectroscopy-based study of balanced transport of charge carriers in hot-air-annealed perovskites. Spectrochimica Acta - Part A: Molecular and Biomolecular Spectroscopy, 2019, 207, 68-72.	3.9	2
67	Synthesis and properties of mono―and diâ€fluoroâ€substituted 2,3â€didodecylquinoxalineâ€based polymers for polymer solar cells. Journal of Polymer Science Part A, 2019, 57, 545-552.	2.3	2
68	Improved Moisture Stability of Perovskite Solar Cells with a Surfaceâ€Treated PCBM Layer. Solar Rrl, 2019, 3, 1800289.	5.8	20
69	Effects of inserting keto-functionalized side-chains instead of imide-functionalized side-chain on the pyrrole backbone of 2,5-bis(2-thienyl)pyrrole-based polymers for organic solar cells. Journal of Photochemistry and Photobiology A: Chemistry, 2019, 371, 387-394.	3.9	5
70	Effects of replacing benzodithiophene with a benzothiadiazole derivative on an efficient wide band-gap benzodithiophene-alt-pyrrolo[3,4-c]pyrrole-1,3(2H,5H)-dione copolymer. Journal of Photochemistry and Photobiology A: Chemistry, 2019, 368, 162-167.	3.9	6
71	Synchronized-pressing fabrication of cost-efficient crystalline perovskite solar cells <i>via</i> intermediate engineering. Nanoscale, 2018, 10, 9628-9633.	5.6	8
72	Photovoltaic polymers based on difluoroqinoxaline units with deep <scp>HOMO</scp> levels. Journal of Polymer Science Part A, 2018, 56, 1489-1497.	2.3	8

#	Article	IF	CITATIONS
73	Break the Interacting Bridge between Eu3+ Ions in the 3D Network Structure of CdMoO4: Eu3+ Bright Red Emission Phosphor. Scientific Reports, 2018, 8, 5936.	3.3	31
74	Blue shift behavior of Eu2+ emission in eulytite-type Sr3La(PO4)3 phosphor based on the release of adjacent Eu3+-induced stress. Journal of Alloys and Compounds, 2018, 742, 159-164.	5.5	30
75	Synthesis and photovoltaic properties of copolymers with a fluoro quinoxaline unit. Journal of Polymer Science Part A, 2018, 56, 821-830.	2.3	18
76	Photoluminescence properties of SrLaMgTaO6 double-perovskite thin film. Journal of Alloys and Compounds, 2018, 755, 67-72.	5.5	3
77	Regioregular dithienosilole- and dithienogermole-based small molecules with symmetric distal/distal orientation of F atoms. Dyes and Pigments, 2018, 155, 7-13.	3.7	4
78	Highly crystalline new benzodithiophene–benzothiadiazole copolymer for efficient ternary polymer solar cells with an energy conversion efficiency of over 10%. Journal of Materials Chemistry C, 2018, 6, 4281-4289.	5.5	31
79	Crystal structure, electronic structure and photoluminescence properties of KLaMgWO6:Eu3+ phosphors. Journal of Luminescence, 2018, 197, 270-276.	3.1	34
80	Two new tercopolymers incorporating electron-rich benzodithiophene and electron-accepting pyrrolo[3,4-c]pyrrole-1,3-dione and difluorobenzothiadiazole derivatives for polymer solar cells. Polymer Bulletin, 2018, 75, 239-253.	3.3	3
81	Colloidal GdVO 4 :Eu 3+ @SiO 2 nanocrystals for highly selective and sensitive detection of Cu 2+ ions. Applied Surface Science, 2018, 433, 381-387.	6.1	21
82	Ca9Na1/3M2(1-)/3(PO4)7:2x/3Eu3+ (M = Gd, Y): A promising red-emitting phosphor without concentration quenching for optical display applications. Journal of Luminescence, 2018, 194, 346-352.	3.1	12
83	The tetravalent manganese activated SrLaMgTaO 6 phosphor for w-LED applications. Materials Research Bulletin, 2018, 97, 115-120.	5.2	38
84	Overcoming Fill Factor Reduction in Ternary Polymer Solar Cells by Matching the Highest Occupied Molecular Orbital Energy Levels of Donor Polymers. Advanced Energy Materials, 2018, 8, 1702251.	19.5	48
85	Thiophene and thieno[3,2-b]thiophene π-bridged pyrrolo[3,4-c]pyrrole-1,3-dione-based wide band-gap polymers for fullerene and non-fullerene organic solar cells. Organic Electronics, 2018, 63, 78-85.	2.6	9
86	Molybdenum substitution induced luminescence enhancement in Gd2W1-Mo O6:Eu3+ phosphors for near ultraviolet based solid-state lighting. Journal of Luminescence, 2018, 202, 97-106.	3.1	26
87	Wide range yellow emission Sr8MgLa(PO4)7: Eu2+, Mn2+, Tb3+ phosphors for near ultraviolet white LEDs. Materials Research Bulletin, 2018, 107, 280-285.	5.2	16
88	Synthesis of Alkyl‣ubstituted Quinoxalineâ€Based Copolymers Along with Photophysical Property Modulation for Polymer Solar Cells. Macromolecular Chemistry and Physics, 2018, 219, 1800117.	2.2	0
89	Bulk Heterojunction-Assisted Grain Growth for Controllable and Highly Crystalline Perovskite Films. ACS Applied Materials & Interfaces, 2018, 10, 31366-31373.	8.0	17
90	Gate-enhanced photocurrent of (6,5) single-walled carbon nanotube based field effect transistor. Carbon, 2018, 139, 709-715.	10.3	3

#	Article	IF	CITATIONS
91	PyrroleN-alkyl side chain effects on the properties of pyrrolo[3,4-c]pyrrole-1,3-dione-based polymers for polymer solar cells. New Journal of Chemistry, 2018, 42, 12045-12053.	2.8	6
92	Kerf-Less Exfoliated Thin Silicon Wafer Prepared by Nickel Electrodeposition for Solar Cells. Frontiers in Chemistry, 2018, 6, 600.	3.6	6
93	The Effect of Charge Compensation on the Luminescence Behavior of Eu ³⁺ -Doped Perovskite CaZrO ₃ Red Phosphor. Nanoscience and Nanotechnology Letters, 2018, 10, 703-708.	0.4	1
94	The role of Yb ³⁺ concentrations on Er ³⁺ doped SrLaMgTaO ₆ double perovskite phosphors. RSC Advances, 2017, 7, 1464-1470.	3.6	39
95	Enhanced photovoltaic performances of bis(pyrrolo[3,4-c]pyrrole-1,3-dione)-based wide band gap polymer via the incorporation of an appropriate spacer unit between pyrrolo[3,4-c]pyrrole-1,3-dione units. Organic Electronics, 2017, 42, 34-41.	2.6	11
96	Improvement of photoluminescence properties of Eu 3+ doped SrNb 2 O 6 phosphor by charge compensation. Optical Materials, 2017, 66, 220-229.	3.6	51
97	The design and synthesis of new double perovskite (Na,Li)YMg(W,Mo)O 6 :Eu 3+ red phosphors for white light-emitting diodes. Journal of Alloys and Compounds, 2017, 716, 56-64.	5.5	84
98	Enhanced efficiency and stability of polymer solar cells using solution-processed nickel oxide as hole transport material. Current Applied Physics, 2017, 17, 1232-1237.	2.4	7
99	Tunable single-phased white-emitting Sr 3 Y(PO 4) 3 :Dy 3+ phosphors for near-ultraviolet white light-emitting diodes. Ceramics International, 2017, 43, 8497-8501.	4.8	43
100	Effective hot-air annealing for improving the performance of perovskite solar cells. Solar Energy, 2017, 146, 359-367.	6.1	20
101	Single-Crystal-like Perovskite for High-Performance Solar Cells Using the Effective Merged Annealing Method. ACS Applied Materials & Interfaces, 2017, 9, 12382-12390.	8.0	41
102	Synthesis and properties of thiophene- and quinoxaline-based random copolymers for organic photovoltaics. Polymer Bulletin, 2017, 74, 2755-2766.	3.3	2
103	Influence of alkaline ions on the luminescent properties of Mn4+-doped MGe4O9 (M = Li2, LiNa and K2) red-emitting phosphors. Journal of Luminescence, 2017, 192, 1072-1083.	3.1	30
104	Structural, vibrational and band gap tunability of lead-free (1Ââ~Âx)NaBiTO3–xBiMnO3 ceramics. Journal of Materials Science: Materials in Electronics, 2017, 28, 18508-18514.	2.2	1
105	Understanding and Tailoring Grain Growth of Lead-Halide Perovskite for Solar Cell Application. ACS Applied Materials & Interfaces, 2017, 9, 33925-33933.	8.0	39
106	Effect of La3+ ion doping on the performance of Eu2+ ions in novel Sr3CeNa(PO4)2SiO4 phosphors. Journal of Alloys and Compounds, 2017, 724, 763-773.	5.5	12
107	Efficient pyrrolo[3,4-c]pyrrole-1,3-dione-based wide band gap polymer for high-efficiency binary and ternary solar cells. Polymer, 2017, 125, 182-189.	3.8	15
108	Dual-Mode Manipulating Multicenter Photoluminescence in a Single-Phased Ba9Lu2Si6O24:Bi3+, Eu3+ Phosphor to Realize White Light/Tunable Emissions. Scientific Reports, 2017, 7, 15884.	3.3	16

#	Article	IF	CITATIONS
109	Tunable up-conversion luminescence from Er3+/Tm3+/Yb3+ tri-doped Sr2CeO4 phosphors. Journal of Luminescence, 2017, 182, 240-245.	3.1	11
110	Effective methods for improving device performances of P-I-N perovskite solar cells. , 2017, , .		0
111	Pyrrolo[3,4-c]pyrrole-1,3-dione Based Wide Band Gap Polymers for Polymer Solar Cells. Journal of Nanoscience and Nanotechnology, 2017, 17, 5556-5561.	0.9	4
112	Synthesis and Characterization of Novel D-A Conjugated Polymers Based on Fluorinated Quinoxaline and Thiophene Series for Polymer Solar Cells. Journal of Nanoscience and Nanotechnology, 2017, 17, 5802-5805.	0.9	1
113	Luminescence and Energy Transfer Process in YNbO ₄ :Bi ³ ⁺ , Sm ³ ⁺ Phosphors. Science of Advanced Materials, 2017, 9, 349-352.	0.7	14
114	Enhancement in the Device Performance of an Organic Field-Effect Transistor Through Thermal Annealing. New Physics: Sae Mulli, 2017, 67, 1180-1186.	0.1	0
115	Imide-linked alkyl chain influence on the properties of pyrrole-based imide-functionalized polymers containing pyrrolo[3,4-c]pyrrole-1,3(2H,5H)-dione and benzodithiophene units for polymer solar cells. Synthetic Metals, 2016, 220, 34-40.	3.9	4
116	Syntheses of pyrimidineâ€based polymers containing electronâ€withdrawing substituent with high open circuit voltage and applications for polymer solar cells. Journal of Polymer Science Part A, 2016, 54, 771-784.	2.3	7
117	Elaboration, Structure and Luminescence of Sphere-Like CaF2:RE Sub-Microparticles by Ionic Liquids Based Hydrothermal Process. Journal of Nanoscience and Nanotechnology, 2016, 16, 1146-1150.	0.9	5
118	Property modulation of ternary copolymer via the diverse arrangements of two different repeating units for polymer solar cells and thin film transistors. Polymer, 2016, 95, 18-25.	3.8	7
119	Benzodithiophene based ternary copolymer containing covalently bonded pyrrolo[3,4-c]pyrrole-1,3-dione and benzothiadiazole for efficient polymer solar cells utilizing high energy sunlight. Organic Electronics, 2016, 38, 283-291.	2.6	8
120	Luminescence and energy transfer in a color tunable CaY ₄ (SiO ₄) ₃ O:Ce ³⁺ , Mn ²⁺ , Tb ³⁺ phosphor for application in white LEDs. RSC Advances, 2016, 6, 79317-79324.	3.6	14
121	Effects of the incorporation of bithiophene instead of thiophene between the pyrrolo[3,4-c]pyrrole-1,3-dione units of a bis(pyrrolo[3,4-c]pyrrole-1,3-dione)-based polymer for polymer solar cells. New Journal of Chemistry, 2016, 40, 10153-10160.	2.8	10
122	Successful incorporation of optical spacer and additive solvent for enhancing the photocurrent of polymer solar cell. Solar Energy Materials and Solar Cells, 2016, 153, 131-137.	6.2	5
123	Effects of the incorporation of an additional pyrrolo[3,4-c]pyrrole-1,3-dione unit on the repeating unit of highly efficient large band gap polymers containing benzodithiophene and pyrrolo[3,4-c]pyrrole-1,3-dione derivatives. Organic Electronics, 2016, 30, 253-264.	2.6	14
124	Synthesis and photoluminescence of Bi ³⁺ ,Eu ³⁺ doped CdWO ₄ phosphors: application of energy level rules of Bi ³⁺ ions. New Journal of Chemistry, 2016, 40, 3552-3560.	2.8	24
125	Conjugated polymers containing pyrimidine with electron withdrawing substituents for organic photovoltaics with high open-circuit voltage. Polymer, 2016, 83, 50-58.	3.8	16
126	6-(2-Thienyl)-4H-thieno[3,2-b]indole based conjugated polymers with low bandgaps for organic solar cells. Synthetic Metals, 2016, 213, 25-33.	3.9	13

#	Article	IF	CITATIONS
127	Synthesis and Photovoltaic Properties of Copolymers with Fluorinated Quinoxaline and Fluorene Moiety. Applied Chemistry for Engineering, 2016, 27, 467-471.	0.2	Ο
128	Enhanced efficiency of bilayer polymer solar cells by the solvent treatment method. Synthetic Metals, 2015, 199, 408-412.	3.9	16
129	Dual-Mode Luminescence with Broad Near UV and Blue Excitation Band from Sr ₂ CaMoO ₆ :Sm ³⁺ Phosphor for White LEDs. Journal of Physical Chemistry C, 2015, 119, 15517-15525.	3.1	116
130	Synthesis and Properties of Copolymer with Carbazole and F-Quinoxaline Units for OPVs. Molecular Crystals and Liquid Crystals, 2015, 620, 100-106.	0.9	3
131	Palladium-Assisted Reaction of 2,2-Dialkylbenzimidazole and Its Implication on Organic Solar Cell Performances. Journal of Physical Chemistry C, 2015, 119, 14063-14075.	3.1	14
132	Crystal structure and two types of Eu3+-centered emission in Eu3+ doped Ca2V2O7. Journal of Luminescence, 2015, 161, 318-322.	3.1	12
133	A red-emitting perovskite-type SrLa(1â^')MgTaO6:xEu3+ for white LED application. Journal of Luminescence, 2015, 167, 381-385.	3.1	53
134	Synthesis and photoluminescence of novel 3D flower-like CaMoO4 architectures hierarchically self-assembled with tetragonal bipyramid nanocrystals. Optical Materials, 2015, 43, 10-17.	3.6	13
135	Property modulation of dithienosilole-based polymers via the incorporation of structural isomers of imide- and lactam-functionalized pyrrolo[3,4-c]pyrrole units for polymer solar cells. Polymer, 2015, 65, 243-252.	3.8	15
136	Opto-electrical, charge transport and photovoltaic property modulation of 2,5-di(2-thienyl)pyrrole-based polymers via the incorporation of alkyl, aryl and cyano groups on the pyrrole unit. Polymer Bulletin, 2015, 72, 1899-1919.	3.3	3
137	Benzodithiopheneâ€Based Broad Absorbing Random Copolymers Incorporating Weak and Strong Electron Accepting Imide and Lactam Functionalized Pyrrolo[3,4]pyrrole Derivatives for Polymer Solar Cells. Macromolecular Chemistry and Physics, 2015, 216, 996-1007.	2.2	12
138	Modulation of the properties of pyrrolo[3,4-c]pyrrole-1,4-dione based polymers containing 2,5-di(2-thienyl)pyrrole derivatives with different substitutions on the pyrrole unit. New Journal of Chemistry, 2015, 39, 4658-4669.	2.8	8
139	Photoluminescence properties, crystal structure and electronic structure of a Sr ₂ CaWO ₆ :Sm ³⁺ red phosphor. RSC Advances, 2015, 5, 89290-89298.	3.6	34
140	Photocurrent enhancement of an efficient large band gap polymer incorporating benzodithiophene and weak electron accepting pyrrolo[3,4â^'c]pyrroleâr'1,3âr'dione derivatives via the insertion of a strong electron accepting thieno[3,4âr'b]thiophene unit. Polymer, 2015, 80, 95-103.	3.8	8
141	Tuning the physical properties of pyrrolo[3,4-c]pyrrole-1,3-dione-based highly efficient large band gap polymers via the chemical modification on the polymer backbone for polymer solar cells. RSC Advances, 2015, 5, 99217-99227.	3.6	12
142	Tandem Solar Cells Made from Amorphous Silicon and Polymer Bulk Heterojunction Sub ells. Advanced Materials, 2015, 27, 298-302.	21.0	18
143	Key chemical parameters related to the width of the charge transfer band and the emission intensity of 5D0→7F2 in Eu3+ doped Ln2O3. Journal of Alloys and Compounds, 2015, 620, 324-328.	5.5	12
144	Efficiency Enhancement in Polymer Solar Cell Using Solution-processed Vanadium Oxide Hole Transport Layer. New Physics: Sae Mulli, 2015, 65, 709-714.	0.1	0

#	Article	IF	CITATIONS
145	Study of Solution-processable Bilayer Polymer Solar Cells. New Physics: Sae Mulli, 2015, 65, 741-746.	0.1	0
146	Simultaneous realization of two approaches to white light in single-component phosphors. Optics Express, 2014, 22, 25500.	3.4	5
147	Pyrrolo[3,4-c]pyrrole-1,3-dione-based large band gap polymers containing benzodithiophene derivatives for highly efficient simple structured polymer solar cells. Journal of Polymer Science Part A, 2014, 52, n/a-n/a.	2.3	9
148	Switchable polarity in polymer solar cells using conjugated polyelectrolyte. Synthetic Metals, 2014, 188, 1-5.	3.9	3
149	Highly efficient imide functionalized pyrrolo[3,4-c]pyrrole-1,3-dione-based random copolymer containing thieno[3,4-c]pyrrole-4,6-dione and benzodithiophene for simple structured polymer solar cells. Journal of Materials Chemistry A, 2014, 2, 20126-20132.	10.3	40
150	Synthesis and Photovoltaic Properties of Copolymer Containing Fused Donor and Difluoroquinoxaline Moieties. Bulletin of the Korean Chemical Society, 2014, 35, 2963-2968.	1.9	3
151	Synthesis and Photovoltaic Properties of Quinoxaline-Based Semiconducting Polymers with Fluoro Atoms. Bulletin of the Korean Chemical Society, 2014, 35, 2245-2250.	1.9	5
152	Correlation Between Lateral Photovoltaic Effect and Conductivity in p-type Silicon Substrates. Bulletin of the Korean Chemical Society, 2013, 34, 1845-1847.	1.9	1
153	Highly transparent polymer light-emitting diode using modified aluminum-doped zinc oxide top electrode. Applied Physics Letters, 2012, 100, 133306.	3.3	9
154	Synthesis and characterization of dimethyl-benzimidazole based low bandgap copolymers for OPVs. Synthetic Metals, 2012, 162, 988-994.	3.9	7
155	Synthesis and characterization of polycyclopentaphenanthrene with carbazole or oxidiazole pendant units. Polymer Journal, 2012, 44, 347-352.	2.7	5
156	Synthesis and characterization of phenathrothiadiazole-based conjugated polymer for photovoltaic device. Synthetic Metals, 2012, 162, 1936-1943.	3.9	5
157	Light-soaking issue in polymer solar cells: Photoinduced energy level alignment at the sol-gel processed metal oxide and indium tin oxide interface. Journal of Applied Physics, 2012, 111, .	2.5	112
158	Regioselective 1,2,3-bisazfulleroid: doubly N-bridged bisimino-PCBMs for polymer solar cells. Journal of Materials Chemistry, 2012, 22, 22958.	6.7	11
159	Anthradithiophene–thiophene copolymers with broad UV–vis absorption for organic solar cells and fieldâ€effect transistors. Journal of Polymer Science Part A, 2012, 50, 4119-4126.	2.3	10
160	Synthesis and characterization of 2H-benzimidazole- and terthiophene-based polymer for organic photovoltaics. Synthetic Metals, 2011, 161, 307-312.	3.9	6
161	Increasing of stability depended on the position of alkoxy group in PPV. Synthetic Metals, 2011, 161, 1186-1193.	3.9	6
162	Syntheses and characterization of new low-band gap polymers containing 4H-cyclopenta[def]phenanthrene unit and 4,7-di(thien-2-yl)-2H-benzimidazole-2-spirocyclohexane for photovoltaic device. Synthetic Metals, 2011, 161, 1336-1342.	3.9	7

#	Article	IF	CITATIONS
163	Color stability of conjugated polymer with difluoro groups in vinylene units. Macromolecular Research, 2011, 19, 753-756.	2.4	1
164	Syntheses and characterization of carbazole based new lowâ€band gap copolymers containing highly soluble benzimidazole derivatives for solar cell application. Journal of Polymer Science Part A, 2011, 49, 369-380.	2.3	23
165	Novel Filmâ€Casting Method for Highâ€Performance Flexible Polymer Electrodes. Advanced Functional Materials, 2011, 21, 487-493.	14.9	88
166	A Thermally Stable Semiconducting Polymer. Advanced Materials, 2010, 22, 1253-1257.	21.0	165
167	Low-bandgap poly(4H-cyclopenta[def]phenanthrene) derivatives with 4,7-dithienyl-2,1,3-benzothiadiazole unit for photovoltaic cells. Polymer, 2010, 51, 390-396.	3.8	35
168	Conjugated copolymers based on dihexyl-benzimidazole moiety for organic photovoltaics. Polymer, 2010, 51, 5385-5391.	3.8	24
169	Efficiency enhancement in polymer optoelectronic devices by introducing titanium sub-oxide layer. Current Applied Physics, 2010, 10, S528-S531.	2.4	11
170	Synthesis and characterization of lowâ€bandgap copolymers based on dihexylâ€2 <i>hâ€</i> benzimidazole and cyclopentadithiophene. Journal of Polymer Science Part A, 2010, 48, 4567-4573.	2.3	23
171	Synthesis and characterization of low-bandgap copolymers based on dihexyl-2H-benzimidazole and terthiophene. Synthetic Metals, 2010, 160, 2618-2622.	3.9	9
172	A low-bandgap alternating copolymer containing the dimethylbenzimidazole moiety. Journal of Materials Chemistry, 2010, 20, 6517.	6.7	68
173	Semiconducting Polymer Photodetectors with Electron and Hole Blocking Layers: High Detectivity in the Near-Infrared. Sensors, 2010, 10, 6488-6496.	3.8	90
174	Bulk heterojunction solar cells with internal quantum efficiency approaching 100%. Nature Photonics, 2009, 3, 297-302.	31.4	3,903
175	Flexible light-emitting three-terminal device with color-controlled emission. Organic Electronics, 2009, 10, 426-431.	2.6	7
176	Novel conjugated polymers employing the binding of polyfluorene derivatives and C60. Synthetic Metals, 2009, 159, 1529-1537.	3.9	9
177	Titanium suboxide as an optical spacer in polymer solar cells. Applied Physics Letters, 2009, 95, .	3.3	131
178	Isomeric iminofullerenes as acceptors in bulk heterojunction organic solar cells. Journal of Materials Chemistry, 2009, 19, 5624.	6.7	42
179	Synthesis and properties of various PPV derivatives with phenyl substituents. Polymer, 2008, 49, 4559-4568.	3.8	15
180	A novel conjugated polymer based on cyclopenta[def]phenanthrene backbone with spiro group. Polymer, 2008, 49, 5643-5649.	3.8	13

#	Article	IF	CITATIONS
181	Novel Electroluminescent PPV Copolymers Containing Si-phenyl and Difluorovinylene Units. Polymer Journal, 2008, 40, 965-970.	2.7	1
182	Stabilized Polymers with Novel Indenoindene Backbone against Photodegradation for LEDs and Solar Cells. Macromolecules, 2008, 41, 7296-7305.	4.8	70
183	Syntheses and Characterization of Alkoxyphenyl-Substituted PCPP with Stabilized Blue Emission and Its Derivatives with Ketone Unit in the Main Chain. Macromolecules, 2008, 41, 8324-8331.	4.8	11
184	Increased Efficiencies of the Copolymers with Fluoro Groups in Vinylene Units. Macromolecules, 2007, 40, 6799-6806.	4.8	18
185	Synthesis and electroluminescent properties of copolymers based on PPV with fluoro groups in vinylene units. Polymer, 2007, 48, 1541-1549.	3.8	21
186	Metallic transport in polyaniline. Nature, 2006, 441, 65-68.	27.8	834
187	Syntheses and properties of electroluminescent polyfluorene-based conjugated polymers, containing oxadiazole and carbazole units as pendants, for LEDs. Polymer, 2005, 46, 12158-12165.	3.8	57
188	Electroluminescence in polymer-fullerene photovoltaic cells. Applied Physics Letters, 2005, 86, 183502.	3.3	67
189	Stabilized Blue Emission from Organic Light-Emitting Diodes Using Poly(2,6-(4,4-bis(2-ethylhexyl)-4H-cyclopenta[def]phenanthrene)). Macromolecules, 2005, 38, 6285-6289.	4.8	70
190	Novel Electroluminescent Polymers with Fluoro Groups in Vinylene Units. Macromolecules, 2004, 37, 6711-6715.	4.8	63
191	Design, Synthesis, and Electroluminescent Property of CNâ^'Poly(dihexylfluorenevinylene) for LEDs. Macromolecules, 2003, 36, 6970-6975.	4.8	71
192	Substituent position-induced color tunability in polymer light-emitting diodes. Applied Physics Letters, 2002, 81, 1732-1734.	3.3	3
193	Color-Tunable Electroluminescent Polymers by Substitutents on the Poly(p-phenylenevinylene) Derivatives for Light-Emitting Diodes. Chemistry of Materials, 2002, 14, 5090-5097.	6.7	37